Polypropylene Nanocomposite Film: A Critical Evaluation on the Effect of Nanoclay on the Mechanical, Thermal, and Morphological Behavior

S. K. Sharma, Ajay K. Nema, S. K. Nayak

Central Institute of Plastics Engineering and Technology, Chennai 600032, Tamil Nadu, India

Received 23 July 2008; accepted 17 May 2009
DOI 10.1002/app.30883
Published online 4 November 2009 in Wiley InterScience (www.interscience.wiley.com).

ABSTRACT: Polypropylene (PP)/clay nanocomposites prepared by melt blending technique using different percentages of clay with and without maleic anhydride grafted PP (MA-PP) were studied. The intercalated and exfoliated structure of nanocomposites was characterized by X-Ray Diffraction (XRD) and transmission electron microscopy (TEM). Because of the typical intercalated and exfoliated structure, the tensile modulus of the nanocomposites were improved significantly as compared to virgin PP. The viscoelastic behavior of the nanocomposites was studied by dynamical mechanical analysis (DMA) and the results showed that with the addition of treated clay to PP there was substantial improvement in storage modulus increases. The thermal stability and crystallization of the PP nanocomposites as studied by differential scanning calorimeter (DSC) and thermo gravimetric analysis (TGA) were also improved significantly compared to PP. © 2009 Wiley Periodicals, Inc. J Appl Polym Sci 115: 3463–3473, 2010

Key words: montmorillonite (MMT); polypropylene maleic anhydride (PP-*g*-MA); dynamical mechanical analysis (DMA); thermo gravimetric analysis (TGA)

INTRODUCTION

Polypropylene is a commodity polymer, which offers best performance characteristics among all thermoplastics. It can be modified with fiber and its fiber reinforced composite compete even with engineering polymers.[1] In such cases, the polymer clay nanocomposites have received research interest because of the significant macroscopic material property enhancements.[2–5] The most interesting aspect of the use of nanofiller is very low amount of filler that has to be added to polymer to the effective enhancement in the properties and they offer attractive potential diversification and application.[6–9] The well ordered intercalated polypropylene/clay nanocomposites can be prepared by direct intercalation in an extrusion process, where the layered clay particles were dispersed homogeneously in polypropylene matrix and intercalated by extended polypropylene chains.[10,11] The most widely used nanoclay is derived from the Na-montmorillonite (MMT), whose 2 : 1 layered silicate structure consists of several stacked layers separated by a charged intergallery.[12–16] Each silicate layer is 0.98 nm thick with lateral dimensions of 400–1000 nm. The sum of the intergallery spacing and an individual silicate layer thickness is referred to as basal spacing, which is $\sim$ 11.7 Å for Na-MMT.[5] To enhance the compatibility between polymers and MMT, cation exchange reaction is frequently performed.[10] The properties of the composites are strongly dependent on the nature of the filler-matrix interface. The control and modification of surface properties of nanoparticles are, therefore, very important. For polyolefins, due to their non-polar nature, it is difficult to make layered silicates delaminate in the polymer matrix. To improve the mechanical properties and other properties, there are many efforts to enhance dispersability of montmorillonite in polyolefin matrix. As the hydrophilic clay is incompatible with polypropylene, compatibilization between the clay and polypropylene is necessary to form stable polypropylene nanocomposites, therefore, the low molecular weight copolymer of polypropylene grafted maleic anhydride (PP-*g*-MA) is often added as a compatibilizer to facilitate intercalation and exfoliation of the organoclay and maximize its interfacial contact with the polymer matrix polymer.[17–25] This systematic study on the effect of clay loading on mechanical and thermal properties of the nanocomposites on film grade of polypropylene was done. The dispersion characteristics of the clay in polypropylene were determined by XRD and TEM. The melting temperature and thermal stability of the nanocomposites were

Correspondence to: S. K. Sharma (sharmask@gmail.com) or S. K. Nayak (drsknayak@yahoo.com) or A. K. Nema (ajaymrc@yahoo.com).

studied by DSC and TGA, respectively, and to study the viscoelastics behavior of the nanocomposites, the DMA was performed.

EXPERIMENTAL

Materials

Commercial grade H030SG PP was obtained from M/s Reliance Industries (India), with MFI 3 g/10 min and specific gravity 0.920 g/cc. The PP-*g*-MA used in this study is maleic anhydride modified polypropylene (PP-*g*-MA), grade Exxelor P01015, obtained from ExxonMobil Chemical (India), with MFI 150 g/10 min at 230°C. The MA level was typically in the range of 0.25–0.50 wt %. The untreated nanoclay Cloisite Na-MMT with specific gravity 2.86 g/cc & gallery spacing 11.7 Å, Cloisite 20A, Cloisite 30B nanoclay with specific gravity 1.77 and 1.98 g/cc and gallery spacing 24.2 and 18.5 Å, respectively, were obtained from M/s Southern Clay (USA). Closite 20A modified with dimethyl, dehydrogenated tallow, quaternary ammonium and has CEC of 95 meq/100 g clay and Closite 30B modified with methyl, tallow, bis-2-hydroxyethyl, quaternary ammonium as surfactant and has CEC of 90 meq/100 g clay.

Preparation of PP nanocomposites by melt blending technique

All nanocomposites were prepared by melt compounding technique using twin screw extruder Berstoff, ZE25 (Germany), equipped with a co-rotating twin screw as the mixing element. The nanoclay dried at 80°C for 4 h in air-circulated oven prior to compounding to remove moisture. The PP layered silicate nanocomposites were prepared by melt mixing of pre-weighed quantities of polypropylene and montmorillonite nanoclay (untreated and treated) with and without PP-*g*-MA. Initially, optimization of screw speed was done with untreated nanoclay to get the maximum shear effect for exfoliated nanocomposites. The high shear and low output will give more residence time for mixing and high shear rate will increase the intergallery spacing between the clay platelets and polymer facilitate to enter in to the galleries of nanoclay. The screw speed was kept constant at 100 rpm and temperature was kept constant at 180–240°C and extruded strands of the molten composites were then water quenched and palletized for all the composition. The test specimens were prepared by template cutting from the film for measurement of mechanical properties. Three different compositions have been prepared with untreated and treated nanoclay with varying percentage of nanoclay from 3, 5, and 7 wt % without PP-*g*-MA with the optimized rotation speed of twin screw extruder. After optimization of the properties without compatibilizer, PP-*g*-MA was used as compatibilizer for treated nanoclay to visualize the effect of PP-*g*-MA in the range of 5, 10, 15, and 20%.

Preparation of PP nanocomposites film

After blending with untreated and treated nanoclay with and without PP-*g*-MA, the PP nanocomposites film was prepared using Dr. Collins multilayer film extruder. The 50 ± 5 micron thickness film was prepared for all the composition. The temperature was constant at 180–240°C for all the composition. Because of the high shear at the time of film preparation, resultant increase in intergallery spacing between the nanoclay and polymer may enter into the galleries nanoclay.

Specific gravity

An analytical balance with a stationary support for an immersion vessel above or below the balance pan was used for specific gravity measurement as per ASTM D 792. The specific gravity of the specimen was calculated as follows.

$$\text{Specific gravity of the specimen} = a/(a + w) - b \quad (1)$$

a = weight of specimen in air
b = weight of specimen in water
w = weight of totally immersed sinker and partially immersed wire.

Melt flow index

Melt flow index of nanocomposites were measured according to ASTM D1238 using LLYODS (UK) apparatus. The applied weight was 2.16 Kg and temperature used was 230°C.

Mechanical properties

Tensile properties were measured using an LR 100K, LLOYDS Instruments (UK), Universal Tester, at crosshead speed 50 mm/min for the virgin PP and PP nanocomposites. The specimen were prepared and conditioned as per ASTM D 618 to analyze various physico-mechanical testing conditioned at 23°C ± 1°C and 55% ± 1% RH. The specimens were cut according to ASTM D 882 from fifty micron film of the compounded samples. Specimen of dimensions 150 × 25 × 0.05 mm was prepared by blown film extrusion. At least five samples were tested for each property and the average values were reported. The mechanical properties results were also expressed in a single decimal and also calculated the standard deviation for all the results and it varies from ±0.55 to ±0.98.

Thermal analysis

Differential scanning calorimeter

Melting points (T_m) of the nanocomposites as well as virgin PP were carried out by Differential Scanning Calorimeter (DSC) instrument using Perkin Elmer. Melting point was measured as per ASTM D 3418. The degree of crystallanity was also calculated for all the composition with reference to the virgin ΔH value. The sample was heated from 50°C to 220°C at the rate of 10°C/min in inert atmosphere. The crystallanity X_c was calculated by relative ratio of enthalpy of fusion per gram of sample to the heat of fusion of PP crystal.[26]

$$\text{Percentage of crystallanity } X_c = (\Delta H_f^{\text{obs}}/\Delta H_f^{\text{o}}) \times 100 \quad (2)$$

Thermo gravimetric analysis

The thermal stability of the nanocomposites was studied to analyze the effect of nanoclay and PP-*g*-MA loading on the thermal stability of the base polymer by using thermogravimetric analyzer (Perkin Elmer). Thermal stability was measured as per ASTM E 967. The samples were heated from 50°C to 600°C at the rate of 20°C/min heating rate under the inert N_2 atmosphere (50 mL/min). The initial degradation temperature, weight loss and final degradation temperature were measured for all the composition and the dosing of nanofiller were also confirmed by TGA residue content.

Rheological analysis

Dynamic mechanical analysis

Specimen of virgin PP and the nanocomposites having dimensions of 23 × 0.5 × 0.05 mm were subjected to DMA NETZSCH 242 (Germany). The measurements were carried out in bending mode of the equipment and corresponding viscoelastics properties were determined as function of temperature. The range used in present investigation was carried from −150°C to 150°C with the heating rate of 10°C under nitrogen flow. The samples were scanned at a fixed frequency of 1 Hz with a static strain of 0.3% and dynamic strain of 0.1%.

X-ray diffraction

Wide angle X-ray diffraction (WXRD) was carried out to examine the basal spacing of the pure clay as well as nanocomposites using XRD instrument model Scifert 2002 (Japan). X-ray diffraction operated at generator voltage = 45 KV, current = 40 mA, and λ = 1.5405 Å. Measurements were recorded at every 0.03° interval.

Morphological characterization

The morphological properties of the nanocomposites were observed by scanning electron microscope (SEM) and Transmission electron microscope (TEM). The state of dispersion of the filler in the polymer blends were assessed by TEM imaging using Philips CM 20 instrument (Canada). Ultra microtome and stained in R_4O_4 vapor to enhance the phase contrast between the PP and nanoclay. For scanning electron microscope (SEM) observation, thin section having fifty micron thickness sample were cut using a glass knife at room temperature to obtain flat surfaces. The samples were observed on a SEM instrument model JEOL 6360 (Japan). The SEM images were analyzed by using the sigma scan pro image analyze software to observed the dispersion of nanoclay and surface properties.

RESULTS AND DISCUSSION

The PP nanocomposites were prepared with 3, 5, and 7% of untreated nanoclay–Na-MMT, treated nanoclay–Cloisite 20A (C20A), Cloisite 30B (C30B). All combinations were prepared with the 5, 10, 15, and 20% PP-*g*-MA. The optimized results only presented where the properties enhancement is at higher side, i.e., 3% treated and untreated clay with 20% PP-*g*-MA.

Optimization of screw speed and percentage of nanoclay

To obtain intercalated/exfoliated nanocomposites, the certain parameters are critical like matrix which is to be act as a reinforced medium with clay should be compatible with clay and other the surfactant group of clay should be compatible with matrix for the homogenous distribution in a matrix and last the PP-*g*-MA should have a correct chemical balance to get the compatibility between clay and matrix and the last the processing parameter should be optimized to get better exfoliation by shear thinning of matrix in presence of clay, probably the rotation speed, through output and temperature of crystallization are controlling factor to get exfoliated PP Nanocomposites.

These parameters are very important to get the higher reinforcing effect at nanolevel without agglomeration of clay. By changing any one of the parameter may lead to give negative effect on synergistic effect on nanoparticle. To optimize the processing parameter, the experiment has been conducted with different screw speed and the same was evaluated in terms of mechanical properties. The PP matrix initially blended with Na-MMT clay at four different screw speeds (i.e., 100 rpm,

TABLE I
Mechanical Properties for Optimization of Screw Speed

S. No.	Composition	Screw speed in rpm	Tensile strength (MPa)	Tensile modulus (MPa)	Elongation (%)
1	PP Virgin	100	12.9	101.3	51.0
2	PP/Nano	100	14.3	131.4	41.0
3	PP/Nano	150	12.9	118.9	39.1
4	PP/Nano	200	11.1	98.9	36.9

150 rpm, and 200 rpm) the property obtained by varying the rotation speed of screw is depicted in Table I

At the screw rotation speed of 100 rpm, the properties enhancement was highest, i.e., around 10–12% which is due to low throughput, low rotation speed, residence time is more inside the twin screw extruder, gives more time to shear. The clay platelets breaking and the polymer are having sufficient time to penetrate into the gallery of platelets. At higher rpm, the residence time inside the twin screw extruder is less thereby shearing effect of screw was not maintained for longer period of time and hence the properties are reduced. The 100 rpm rotation speed and 220°C temperature kept constant for all other composition.

The PP nanocomposites were prepared with 3, 5, and 7 wt % of untreated nanoclay Na-MMT, treated nanoclay C20A, C30B. The optimized result was shown in Table II and properties enhancement was at higher side for nanocomposites containing 3% nanoclay and the same percentage of nanoclay kept constant for further studies. All the combinations were prepared with the 5, 10, 15, and 20 wt % compatibilizer. The optimized results are only presented here where the properties enhancement is at higher side, i.e., 3 wt % treated and untreated clay with 20 wt % PP-*g*-MA compatibilizer.

Effect on physical properties

Specific gravity

Addition of 3% untreated and treated clays in PP matrix specific gravity shows marginal increment.[27] The specific gravity values were shown in Table III.

TABLE II
Mechanical Properties for Optimization Percentage of Nanoclay

S. No.	Composition	Tensile strength (MPa)	Tensile modulus (MPa)	Elongation (%)
1	PP Virgin	12.9	101.3	51.0
2	PP/Nano 3%	16.1	151.3	36.0
3	PP/Nano 5%	14.1	129.1	38.5
4	PP/Nano 7%	13.1	101.3	40.8

The formation of intercalated/exfoliated structure in PP nanocomposites is also proved by specific gravity measurement. On addition of treated clay with PP-*g*-MA, the specific gravity were increased due to the nucleating effect of PP-*g*-MA and reinforcing effect of nanoclay.

Melt flow index

MFI has marginal effect and it was declining due to addition of clays, on further addition of compatibilizer due to plasticization effect of PP-*g*-MA showing increase in MFI values, generate low molecular weight species. The MFI values were shown in Table III.

Mechanical properties

Tensile properties

The PP was blended with treated and untreated nanoclay with and without PP-*g*-MA and these nanocomposites films were prepared. Mechanical properties were evaluated on keeping the parameters constant like rotation speed and crystallization temperature. The Na-MMT was showing the marginal improvement due to the incompatibility of Na-MMT with PP matrix. The incompatibility arises due to non-polar nature of PP and unavailability of surfactant on surface of nanoclay. The mechanical properties of PP nanocomposites were shown in Table IV.

The nanocomposites subjected to shearing at the time of compounding and once again at the time of preparation of nanocomposites film. The enhancement in properties mainly depends on compatibility dispersion of nanoclay, orientation of nanoclay in proper direction to get a better reinforcement. These effects are reflecting in case of treated nanoclay where the tensile properties were increased to 25% for 3% C20A and 20% enhancement for 3% C30B. On addition of PP-*g*-MA further the properties enhancement was observed due to plasticization effect of PP-*g*-MA, makes matrix to diffuse into the silicate layers of nanoclay.[28–30] Around 50%

TABLE III
Physical Properties of PP Nanocomposites

S. No.	Composition	Specific gravity (g/cm^3)	MFI (g/10 min)
1	PP VIRGIN	0.910	3.00
2	PP 3% Na-MMT	0.922	2.55
3	PP 3% C20A	0.911	2.97
4	PP 3% C30B	0.917	2.78
5	PP 3% C20A, 20% PP-*g*-MA	0.918	3.20
6	PP 3% C30B, 20% PP-*g*-MA	0.925	2.99

TABLE IV
Mechanical Properties of PP Nanocomposites

S. No.	Composition	Tensile strength (MPa)	Tensile modulus (MPa)	Elongation at break (%)
1	PP Virgin	12.9	101.3	51.0
2	PP 3% Na-MMT	14.3	131.4	41.0
3	PP 3% C20A	17.2	152.5	49.0
4	PP 3% C30B	16.0	140.9	37.1
5	PP 3% C20A, 20% PP-*g*-MA	26.6	266.8	59.4
6	PP 3% C30B, 20% PP-*g*-MA	23.9	221.9	54.6

enhancements in tensile strength were observed in case of PP 3% C20A with 20% PP-*g*-MA whereas, in case of PP 3% C30B with 20% PP-*g*-MA there was 40% enhancement was observed confirming exact balance of polarity of matrix and clay and showing a better reinforcement effect of PP with nanoclay in presence of PP-*g*-MA.[31]

Thermal analysis

Differential scanning calorimeter

To investigate the effect of dispersion of nanoclay on the degree of crystallinity [X_c (%)] DSC analysis was carried out. The curve for PP and the nanoclay with and without PP-*g*-MA is depicted in Figure 1, and the results of ΔH and percentage of crystallinity is reported in Table V.

The virgin PP crystallanity was determined using a ΔH° of 165 J/g for 100% crystalline PP.[26] Addition of nanoclay due to the dispersion and infusion of matrix into the gallery of nanoclay gives more reinforcement and this reinforcement favors when chemical compatibility of nanoclay matched with matrix. This could be the reason for increase in the melting point on the addition of treated nanoclay. Further, on addition of PP-*g*-MA the diffusion of matrix into the galleries of nanoclay is pronounced and there by further increase of reinforcement and melting point as well. The presence of nanoclay platelets promotes the heterogeneous nucleation and increase in crystallinity rate resultant increase in crystalline. Wang et al.[11] reported PP-*g*-MA act as nucleating agent and lead to an increase in crystallization. On addition of clay, the crystallanity increased, on further addition of PP-*g*-MA, the crystallanity increased due to nanoclay

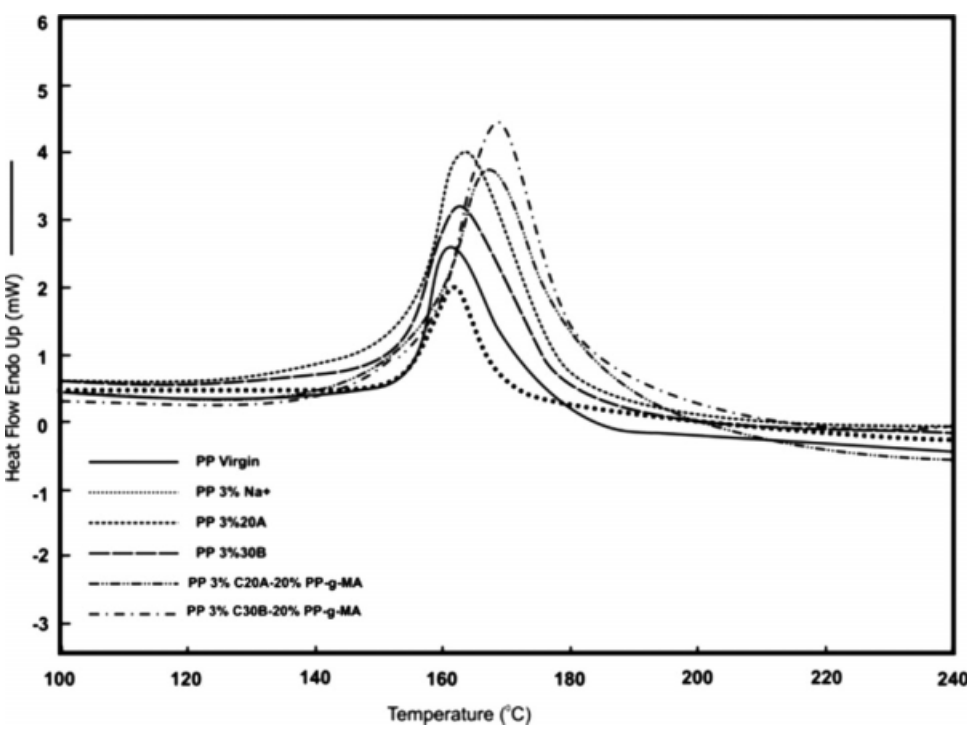

Figure 1 DSC thermograms of PP nanocomposites.

TABLE V
DSC Derived Parameters for PP Nanocomposites

S. No.	Composition	T_m (°C)	X_c (%)	ΔH_f (J/g)
1	PP VIRGIN	161.6	100	165.0
2	PP 3% Na-MMT	161.7	70.5	116.3
3	PP 3% C20A	162.3	71.6	118.3
4	PP 3% C30B	162.1	71.5	117.9
5	PP 3% C20A, 20% PP-*g*-MA	168.1	75.8	125.1
6	PP 3% C30B, 20% PP-*g*-MA	166.4	73.1	120.7

and PP-*g*-MA acting as a nucleating agent.[32–34] The PP 3% C20A with 20% PP-*g*-MA showed increase in crystallanity from 70.24 to 75.83%. An increase in crystallanity to high as 75.83% in 3% C20A with 20% PP-*g*-MA, it is hypothesized that the clay platelets act as nucleating agent, increase the number of sites for crystal growth. The decline in crystallanity at higher loading may be from reduced mobility, thus hindering crystal growth.

Thermogravimetric analysis

The TGA analysis of nanocomposites containing treated/untreated, PP-*g*-MA and non-PP-*g*-MA nanocomposites shown in Figure 2, and the data derived from the graph is presented in Table VI. On addition of Na-MMT there was a marginal increase in thermal stability but on addition of treated clay, the drastic improvement in thermal stability was observed, i.e., increase of around 64°C. On addition of 20% PP-*g*-MA with C20A treated nanoclay around 90°C, enhancements in thermal stability was observed. The drastic improvement in thermal stability would be due to the confinement of the single nanoparticles in 1 nm^3 volume showing existence of single nanoparticle effect. On further addition of clay percentage, the possibility of existence of confine and reinforced nanoparticles is less and the particle may agglomerate. The other reason attributed to the formation of high performance carbonaceous silicate char build up on the surface that insulate the underline material and shows the escape of volatile products generated during the decomposition.[35] The above two possible reason for increase in thermal stability of around 90°C explained the formation of exfoliated structure in presence of PP-*g*-MA. The

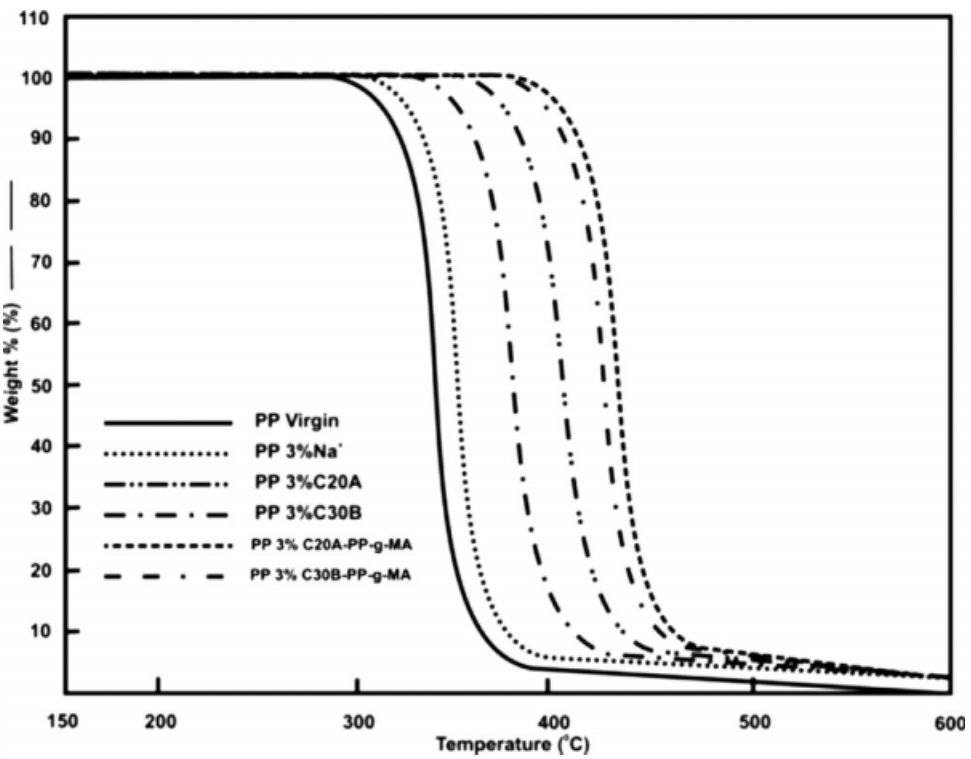

Figure 2 TGA curves of PP nanocomposites.

TABLE VI
TGA Values of PP Nanocomposites

S. No.	Composition	Initial degradation temperature Td_m (°C)	Temperature at max degradation Td_m (°C)	Residue content (%) at 600°C
1	PP VIRGIN	302	385	–
2	PP 3% Na-MMT	313	398	2.98
3	PP 3% C20A	366	454	2.95
4	PP 3% C30B	342	429	2.96
5	PP 3% C20A, 20% PP-*g*-MA	393	480	3.1
6	PP 3% C30B, 20% PP-*g*-MA	387	472	3.0

presences of nanofiller were also confirmed by the residue content. On analysis it was found that it was maintained around 3% in all the compositions.

Dynamical mechanical analysis

The DMA curve of treated and untreated, with and without PP-*g*-MA is depicted in Figure 3, and the data derived is shown in the Table VII. DMA analysis shows that on addition of clay the storage modulus is increased due to the intercalation at nanolevel. The higher the residence time in the screw during compounding in these nanocomposites transmits higher shear stress to the molten polymer, responsible for good dispersion of nanoclay, and remarkable improvement in stiffness. The storage modulus of unfilled polymer in the presence of PP-*g*-MA is reduced[11] due to plasticization effect of PP-*g*-MA.

The storage modulus (E') is the measure of stiffness or the range where the elastic property is higher. The higher the range, the higher will be the stiffness and load bearing capability of nanocomposites. On addition of untreated nanoclay, the modulus increased due to the partial reinforcement, restricting the mobility of the chain segment. On addition of the treated nanoclay, the storage modulus increased and further reduced when PP-*g*-MA was added. Addition of PP-*g*-MA lead to give lower storage modulus to the treated nanoclay PP nanocomposites[36] but the storage modulus of treated nanocomposites is higher than that of the PP virgin which is probably owing to better dispersion of clay. Damping Coefficient (Tan δ) is an indicator of how efficiently a material loses energy to molecular rearrangements and internal friction. Tan δ peaks below the T_g of a material on a DMA curve are often used to determine how well a material will stand up to impact. By analyzing Tan δ for different composition, the T_g value comedown from −10°C to 7°C and 3.7°C for C20A and C30B, respectively. On addition of PP-*g*-MA, further increase from −10°C to 12°C due to the reinforcement[37] and polymer may enter

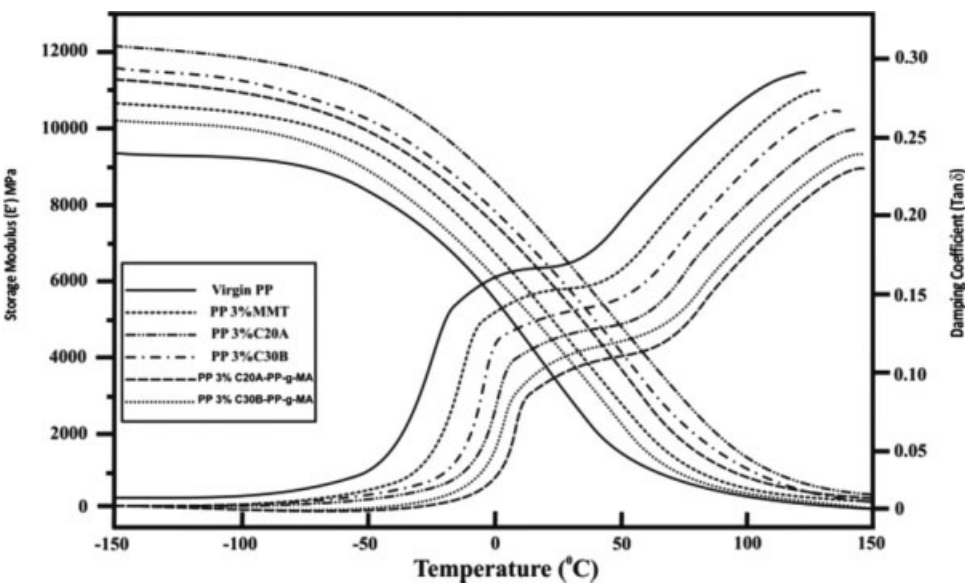

Figure 3 Dynamic mechanical analysis curves of PP nanocomposites.

TABLE VII
Dynamic Mechanical Properties of PP Nanocomposites

S. No.	Composition	Storage Modulus (MPa)	T_g (°C)
1	PP VIRGIN	9.76×10^3	−10.0
2	PP 3% Na-MMT	1.08×10^3	−3.2
3	PP 3% C20A	1.22×10^4	7.0
4	PP 3% C30B	1.17×10^4	3.7
5	PP 3% C20A, 20% PP-*g*-MA	1.14×10^4	12.1
6	PP 3% C30B, 20% PP-*g*-MA	1.02×10^4	8.3

in to the galleries of silicate layer and thereby expand the inter galleries spacing resulted in exfoliated structure. The nanoclay and PP-*g*-MA acting as nucleating agent and the increase in percentage of crystallinity was observed resulted decrease in amorphous region and increase in T_g in presence of PP-*g*-MA as reinforcement increases and molecular mobility decreases. The increase in the storage modulus value could be due to increase in the crystalline domain size in presence of PP-*g*-MA.

X-Ray diffraction

XRD pattern of Na-MMT and modified C20A and C30B is shown in Figure 4. XRD curve of Na-MMT, C20A, and C30B reinforced with PP matrix with and without PP-*g*-MA is shown in Figure 5, and the corresponding 2θ value and *d*-spacing shown in Table VIII. The XRD of Na-MMT has a single peak at about 7.98°, corresponding to a basal spacing of 11.1 Å. The surface modification of these unmodified clay lead to give lower degree angle at about 2.94° for 20A and 5.61° for 30B corresponding to a basal spacing of 30.0 Å and 15.73 Å, respectively.

The morphological structures of nanocomposites are further studied by XRD. The XRD of Na-MMT, treated clay C20A, C30B with 20%PP-*g*-MA is shown in Figure 4. The differential peak 2θ value and *d*-spacing is given in Table VII. On addition of untreated clay with PP matrix, the 2θ value shifted to the lower angle from 7.98° to 6.26° and the corresponding *d*-spacing was increased from 11.1 Å to 32.1 Å. The shifting was towards lower angle with respect to pure MMT on addition of treated clay.[38]

It was observed that C20A diffraction peak shifted from 7.98° to 2.75° the *d*-spacing increased from 11.1 Å to 32.1 Å. The similar observation was recorded for C30B. The shift of the peak related to the distance between the clay platelets. This shows the infusion of polymer into the galleries of silicate layer and forming an intercalated system.[38] This was again confirmed with TEM results.

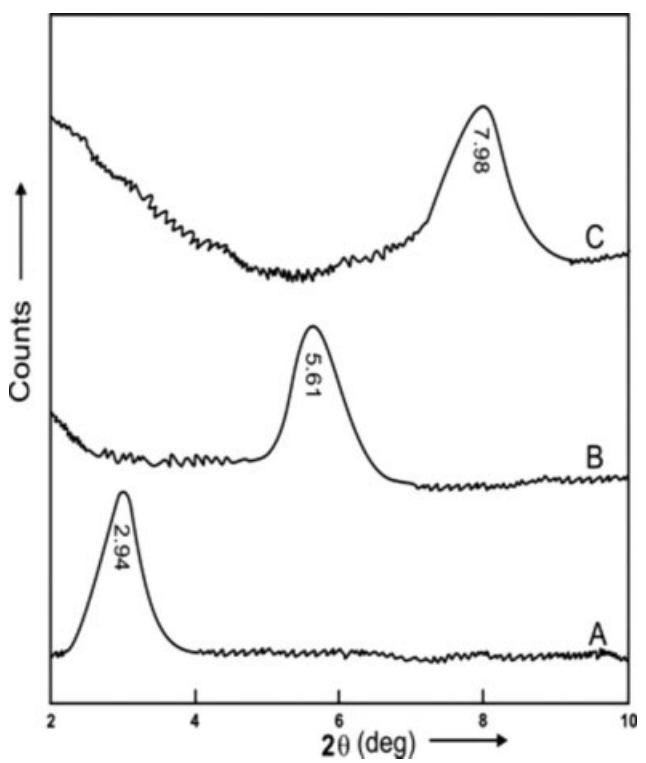

Figure 4 XRD pattern (A: C20A, B: C30B, and C: Na-MMT clays).

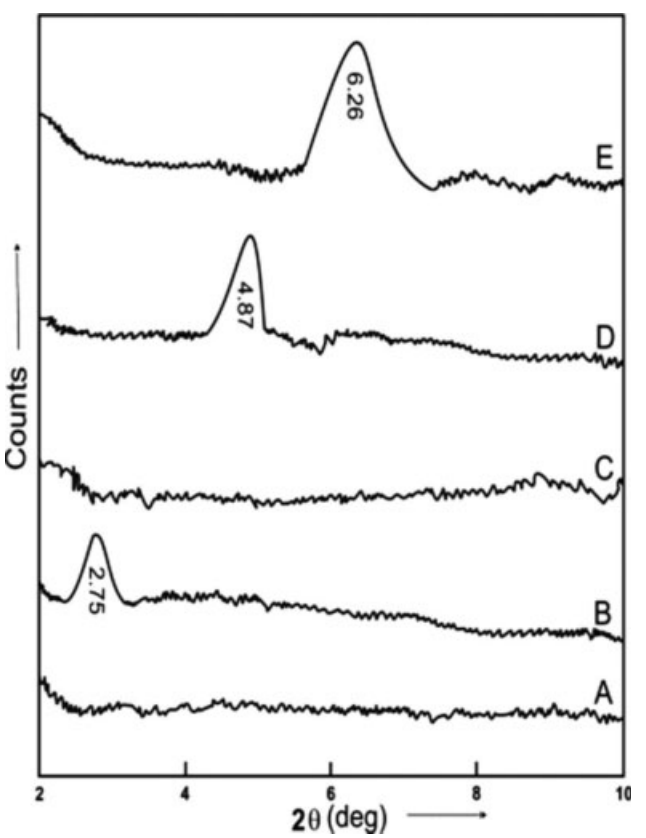

Figure 5 XRD pattern of Na-MMT and treated C20A and C30B clays with PP and PP-*g*-MA.

TABLE VIII
XRD Results of PP Nanocomposites

S. No.	**Code**	Composition	2θ (°)	*d*-spacing (Å)
1	A	PP 3% C20A, 20% PP-*g*-MA	–	–
2	B	PP 3% C20A	2.75	32
3	C	PP 3% C30B, 20% PP-*g*-MA	–	–
4	D	PP 3% C30B	4.87	18.1
5	E	PP 3% Na-MMT	6.26	13.9

On addition of PP-*g*-MA in treated clay/PP matrix the lower angle peak disappears further confirming the intercalated system converted to fully exfoliated system.[39,40] This phenomenon was observed for both C20A and C30B with 20% PP-*g*-MA.

Scanning electron microscopy

SEM observation showed that the clays were dispersed into the PP matrix in the form of large and small tactoid.[28] It was very difficult to estimate the size of the tactoid because the aggregates are non-isometric and randomly dispersed in the matrix.

The size of the observed tactoid is strongly depending on the orientation of the particles. However, the surface of the samples and the dispersion quality of clays, such as aggregates concentration was observed.[41] Figure 6(a–e) are the SEM micrographs of the mixtures containing Na-MMT, C20A,

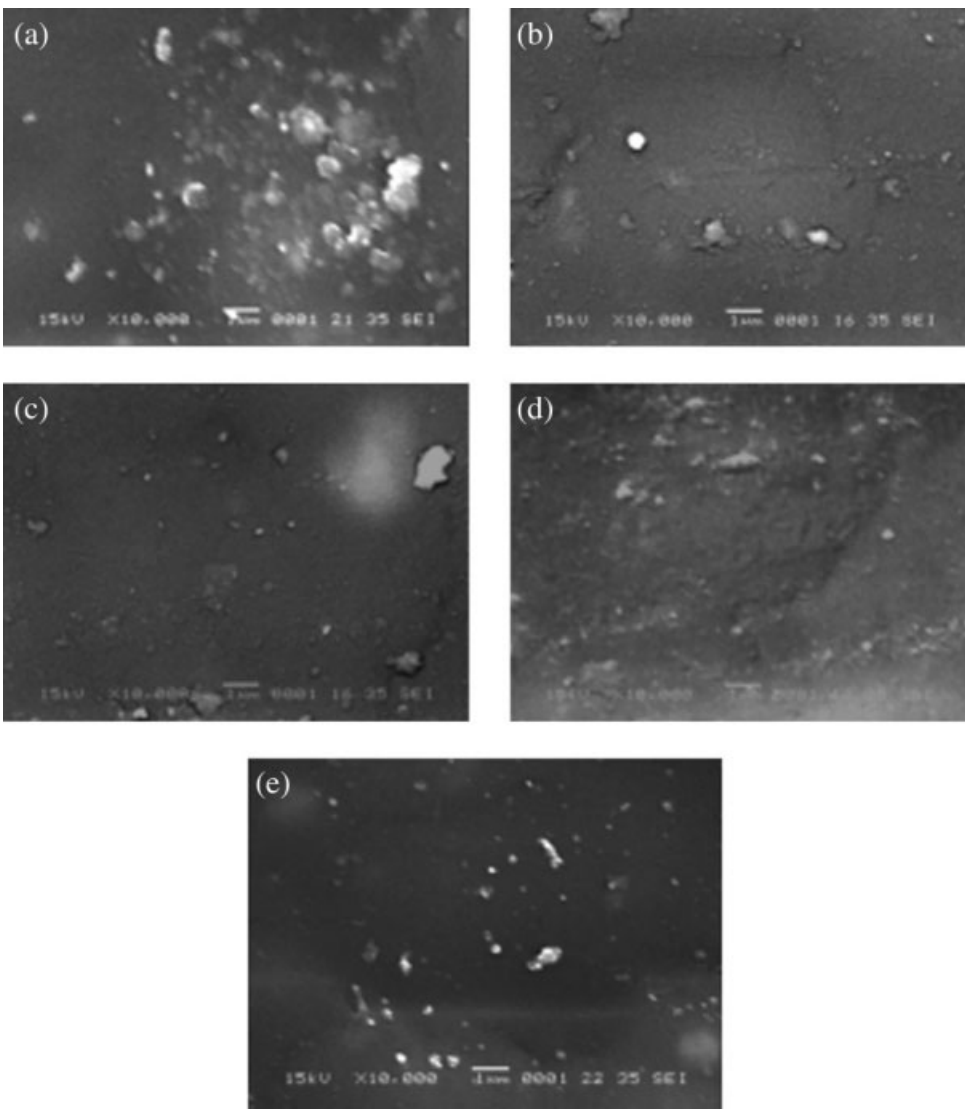

Figure 6 Scanning electron microscopy images of PP nanocomposites. (a) PP 3% Na-MMT, (b) PP 3% C20A, (c) PP 3% C30B, (d) PP 3% C20A, 20% PP-*g*-MA, and (e) PP 3% C30B, 20% PP-*g*-MA.

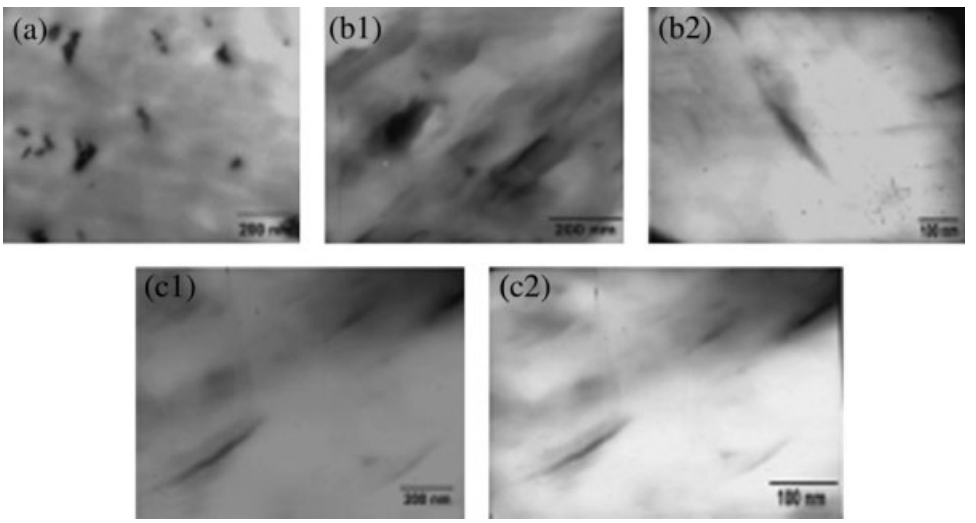

Figure 7 TEM images of PP nanocomposites. (a) PP 3% Na-MMT, (b1) PP 3% C30B, (b2) 20% PP-*g*-MA, and (c1) PP 3% C20A, (c2) 20% PP-*g*-MA.

and C30B clay, respectively. In Figure 6(a) it was observed that dispersion of clay was not uniform and the smallest lateral dimension of clay tactoid were present. However, in Figure 6(d,e), i.e., PP-*g*-MA based nanocomposites, the nanoclay uniformly dispersed in the polymer matrix and the SEM magnification shows the intercalated/exfoliated clay platelets, to confirm the intercalated/exfoliated structure the XRD and TEM analysis were carried out and this analysis is also useful to study the extent of intercalation/exfoliation obtained by the nanocomposites. Therefore, the surface treatment for nanoclay is very important to improve the affinity between the nanoclay and the matrix and to break down the large tactoid. This can be attributed to the ability of surface treatment in reducing particle–particle attraction and promoting the expansion of the gallery distance between clay sheets.[11]

Transmission electron microscopy

The extent of intercalation and exfoliation of nanocomposites is shown in Figure 7. The untreated clay without PP-*g*-MA showing clay aggregates at micrometer level and no silicate layer was dispersed showing as a bundle [Fig. 7(a)]. Addition of treated clay along with PP-*g*-MA shows clay dispersed at micrometer level due to swelling effect of PP-*g*-MA. The PP-*g*-MA reduced the viscosity of the matrix and penetrate into the galleries of silicate layer, showing high amount of swelling. This phenomenon will give the increase in interlayer spacing of the clay platelets and higher reinforcement at micro level. This result was also confirmed with XRD results when there was a disappearance of peak was evident. On the addition of treated clay along with PP-*g*-MA the polarity difference is exactly matching for 20% PP-*g*-MA and 20% PP-*g*-MA showing a fully exfoliated structure, these were further confirmed with XRD results. On further addition of PP-*g*-MA, the aggregate size of PP-*g*-MA increase and give aggregation at micrometer level. For the nanocomposites containing C30B clay the polarity difference is not exactly matching with system, intercalates obliquely exfoliated. This is the proof of misbalance of polarity in the system generate in C30B containing system. This structure again confirmed the expansion of intergallery space of silicate layer in presence of PP-*g*-MA.

CONCLUSIONS

This study was intended to see the effect of surfactant, PP-*g*-MA; processing condition to get exfoliated PP nanocomposites film. The film was clear and the data are also confirming the increase of properties like mechanical and thermal and indicate that the reinforcement of clay is happening at nanolevel. The study was also indent to the effect of surfactant, percentage of clay, percentage of compatibilizer and processing parameters like screw, rotor speed, shear rate, residence time. The orientation of the clay while processing in the presence of PP-*g*-MA is very high and indicates better interaction of PP-*g*-MA and silicate layer at nanolevel. The fully exfoliated system was formed with 5 wt % C20A with 20 wt % PP-*g*-MA; this combination was having no polarity difference of maleic anhydride clay and matrix to form exfoliated nanocomposites. On the increase of polarity of nanoclay again, the property reduction was observed in case of C30B PP-*g*-MA system. The exfoliation is confirmed with XRD and TEM results

for C20A and 20% PP-*g*-MA. The XRD and TEM results of this combination proved that in presence of compatibilizer the system was fully exfoliated. The enhancement in mechanical properties, impact properties, along with thermal stability of the nanocomposites proving that exfoliated nanocomposites was formed. The chemical compatibility of nanoclay with matrix, percentage of nanoclay, percentage of polar group in PP-*g*-MA, processing condition (i.e., shear rate, residence time, and temperature) should be optimized. On the change of any one of the component lead to give negative effect on the properties, this may due to chain scissioning due to grafting, filler–filler interaction, and polarity difference between clay and polymer.

References

1. Moet, A. S.; Akelah, A. Mater Lett 1993, 18, 97.
2. Vaia, R. A.; Jandt, K. D.; Kramer, E. J.; Giannelis, E. P. Macromolecules 1995, 28, 8080.
3. Moorti, R. K.; Vaia, R. A.; Giannelis, E. P. Chem Mater 1996, 8, 1728.
4. Giannelis, E. P.; Krishnamoorti, R.; Manias, E. Adv Polym Sci 1999, 138, 107.
5. Ray, S. S.; Okamoto, M. Polym Sci 2003, 28, 1539.
6. Kawasumi, U. A.; Kojima, M.; Okada, Y.; Kurauchi, A.; Kamigaito, T. J Mater Res 1993, 8, 1174.
7. LeBaron, P. C.; Wang, Z.; Pinnavaia, T. J Appl Clay Sci 1999, 15, 11.
8. Alexandre, M.; Dubois, P. Mater Sci Eng 2000, 28, 1.
9. Okamoto, M.; Morita, S.; Kotaka, T. Polymer 2001, 42, 2685.
10. Hasegawa, N.; Okamoto, H.; Kato, M.; Usuki, A. J Appl Polym Sci 2000, 78, 1981.
11. Wang, Y.; Feng, B.; Chen, K.; Wu, C. Polymer 2004, 93, 100.
12. Ma, J. S.; Qi, Z. N.; Hu, Y. L. J Appl Polym Sci 2001, 82, 3611.
13. Manias, E.; Touny, A.; Wu, L.; Strawkecher, K.; Lu, B.; Chung, T. C. Chem Mater 2001, 13, 3516.
14. Kato, M.; Usuki, A.; Okada, A. J Appl Polym Sci 1997, 66, 1781.
15. Oya, A.; Kurokawa, Y.; Yasuda, H. J Mater Sci 2000, 35, 1045.
16. Peter, R.; Hansjorg, N.; Stefen, K.; Rainer, B.; Ralf, T.; Rolf, M. Macromol Mater Eng 2000, 275, 8.
17. Usuki, A.; Kato, M.; Okada, A.; Kurauchi, T. J Appl Polym Sci 1997, 63, 137.
18. Southern Clay Products Inc. Available at: www.nanoclay.com.
19. Giannelis, E. P.; Krisnamoorti, R.; Manias, M. Adv Polym Sci 1999, 138, 107.
20. Hambir, S.; Bulakh, N.; Jog, J. P. Polym Eng Sci 2002, 42, 1800.
21. Wang, S.; Hu, Y.; Zhong Kai, Q.; Wang, Z.; Chen, Z.; Fan, W. Mater Lett 2003, 57, 2675.
22. Ton-That, M. T.; Perrin-Sarazin, F.; Cole, C. K.; Bureau, M. N.; Denualt, J. Polym Eng Sci 2004, 44, 1212.
23. Usuki, A.; Kato, M.; Okada, A.; Kurauchi, T. J Appl Polym Sci 1997, 63, 137.
24. Hasegawa, N.; Kawasumi, M.; Kato, M.; Usuki, A.; Okada, A. J Appl Polym Sci 1998, 67, 87.
25. Liu, X.; Wu, Q.; Berglund, L. A.; Lindberg, H.; Fan, J.; Qi, Z. J Appl Polym Sci 2003, 88, 953.
26. Moore, E. P., Jr. Polypropylene Handbook; Hanser Gardner: Cincinnati, 1996.
27. Carter, L.; Hendricks, J. G.; Bolley, D. S. US Pat. 2,531,396, 1950.
28. Yuanxin, Z.; Rangari, V.; Mahfuz, H.; Jeelani, S.; Mallick, P. K. Mater Sci Eng A 2005, 402, 109.
29. Kawasumi, M.; Hasegawa, N.; Kato, M.; Usuki, A.; Okada, A. Macromolecules 1997, 30, 6333.
30. Zheng, H.; Zhang, H. Y.; Peng, Z.; Zhang, Y. J Appl Polym Sci 2004, 92, 638.
31. Xu, M.; Hu, Sh.; Zhang, X.; Guan, J. Polym Commun Chin 1981, 5, 339.
32. Via, R. A.; Saure, B. B.; Tse, O. K.; Giannelis, E. P. J Polym Sci Polym Phys 1997, 35, 59.
33. Jang, B. Z. J Appl Polym Sci 1984, 29, 4377.
34. Jang, B. Z. J Appl Polym Sci 1985, 30, 2485.
35. Modesti, M.; Lorenzetti, A.; Bon, D.; Besco, S. Polymer 2005, 46, 10237.
36. Lertwimolnun, W.; Vergnes, B. Polymer 2005, 46, 3462.
37. Szazdi, L.; Pukanszky, B.; Foldes, E., Jr.; Pukanszky, B. Polymer 2005, 46, 8001.
38. Tange, Y.; Yuan, H.; Song, L.; Ruowen, Z.; Zhou, G.; Zuyao, C.; Weicheng, F. Polymer 2003, 82, 127.
39. Lee, H.-s.; Paula, D.; Fasulo, W.; Rodgers, R.; Paul, D. R. Polymer 2005, 46, 11673.
40. Perrin-Sarazil, F.; Ton-That, M.-T.; Bureau, M. N.; Denault, J. Polymer 2005, 46, 11624.
41. Galgali, G.; Ramesh, C.; Lele, A. Macromolcules 2001, 34, 852.